Convective Burning in Solid-Propellant Cracks

K. K. Kuo,* A. T. Chen,† and T. R. Davis‡
The Pennsylvania State University, University Park, Penn.

Transient combustion processes inside solid-propellant cracks can significantly affect the performance of a rocket motor. A comprehensive theoretical model has been developed to study the gas dynamics, heat transfer, and flame spreading phenomena within a single isolated crack. Calculations obtained from the theoretical model revealed that the internal pressurization rate, pressure gradient, and flame propagation velocity in propellant cracks decrease as the gap width increases, the rocket chamber pressurization rate decreases, and the propellant gasification temperature increases. Additionally, the predicted flame spreading was found to decelerate in a region near the crack tip; this phenomena has been experimentally observed by others. A laboratory-size combustion chamber has been designed to establish a fundamental data base in propellant crack combustion and to verify the predicative capability of the theoretical model. Preliminary experimental data, obtained in wide cracks (~0.1 cm) for relatively low chamber pressurization rates, closely compares with theoretical predictions.

Nomenclature

A_p = cross-sectional area of the crack, cm^2
B_x = body force, g_f/g
b = co-volume, cm^3/g
c = speed of sound, cm/s
c_p = specific heat at constant pressure, cal/g-K
d_h = hydraulic diameter of the crack, cm
E = total stored energy, cal/g
g = acceleration of gravity, conversion factor, $g\text{-}cm/g_f\text{-}s^2$
$\bar{h}_c$ = local convective heat-transfer coefficient, $cal/cm^2\text{-}s\text{-}K$
$\bar{h}_{cp}$ = local convective heat-transfer coefficient over the propellant surface, $cal/cm^2\text{-}s\text{-}K$
$\bar{h}_{cw}$ = local convective heat-transfer coefficient over nonpropellant port wall, $cal/cm^2\text{-}s\text{-}K$
h_f = enthalpy of combustion gas at adiabatic flame temperature, cal/g
J = mechanical equivalent of heat, $g_f\text{-}cm/cal$
$\mathcal{P}_b$ = burning perimeter, cm
$\mathcal{P}_w$ = wetted perimeter of the port, cm
p = static pressure, g_f/cm^2
R = specific gas constant for the combustion gases, $g_f\text{-}cm/g\text{-}K$
r_b = burning rate of the solid propellant, including the erosive burning contribution, cm/s
T = temperature (without subscript, static gas temperature), K
T_f = adiabatic flame temperature of the solid propellant, K
T_{pi} = initial propellant temperature, K
T_{ps} = propellant surface temperature, K
T_{ws} = nonpropellant wall surface temperature, K
t = time, s
u = gas velocity, cm/s
V_{gf} = velocity of propellant gas at the burning surface, cm/s
x = axial distance from propellant crack opening, cm
x_L = position at the end of crack, cm
x_p = axial distance along the crack at which propellant begins, cm
y = perpendicular distance from the propellant surface into the solid, cm
α = thermal diffusivity, cm^2/s
γ = ratio of specific heats
λ = thermal conductivity, cal/cm-s-K
μ = gas viscosity, g/cm-s (poise)
ρ = density (without subscript, gas density), g/cm^3
τ_w = shear stress on the port wall, g_f/cm^2
τ_{xx} = normal viscous stress, g_f/cm^2
Θ_w = angle measured, in a counterclockwide direction, at the lower side of the propellant, degree

Subscripts

i = initial value
pr = solid propellant (condensed phase)
c = rocket chamber

I. Introduction

VOIDS, cracks, or fissures in solid-propellant grains have been responsible for the failure of many rocket motors to meet acceptance specifications.[1] These defects may originate as a result of the manufacturing process, damage received during handling and transportation, and chemical aging or thermal stresses incurred during storage. However, even though the propellant grain is free of cracks before firing, there is a possibility that cracks can form in regions of large stress concentration during rocket motor operation. Combustion within a crack can lead to a pressure buildup sufficient to cause further propagation of the crack, resulting in an unexpected increase in the surface available for burning. Thus, there has been much concern among rocket motor designers as to the extent that crack combustion may contribute to catastrophic failure.

Prior to this study, no comprehensive theory has been developed to explain the transient combustion of propellant within cracks, due to the complexity of several interacting phenomena. Ignition and combustion processes in solid propellant cracks generally involve 1) penetration of combustion product gases into the crack cavity, 2) convective heating of the propellant surface to ignition and transient conduction within the solid propellant, 3) pressure wave phenomena in the longitudinal direction of the crack, 4) flame spreading along the crack, 5) cavity pressurization due to gasification of the solid propellant, 6) flow reversal due to the chamber pressurization, 7) deformation of the crack geometry due to burning and pressure loading, and 8) propagation of the crack tip due to gasification and stress loading.

Presented as Paper 77-14 at the AIAA 15th Aerospace Sciences Meeting, Los Angeles, Calif., Jan. 24-26, 1977; submitted Oct. 25, 1977; revision received Feb. 23, 1978. Copyright © American Institute of Aeronautics and Astronautics, Inc., 1977. All rights reserved.

Index category: Combustion Stability, Ignition, and Detonation.

*Associate Professor, Department of Mechanical Engineering. Member AIAA.

†Graduate Student; presently working at Union Carbide Corp., S. Charleston, W. Va. Member AIAA.

‡Graduate Student; presently working at Bethlehem Steel Corp., Bethlehem, Pa.

In addition to these complicated and interrelated phenomena, there are many other important factors that can influence the crack combustion process. These factors include 1) the initial geometry of the crack, 2) the variation of rocket chamber conditions, 3) erosive burning phenomena due to high gas velocities, 4) dynamic burning phenomena due to rapid pressure transients, 5) physicochemical properties of the propellant, and 6) the initial temperature of the propellant.

Although the overall process of transient crack combustion is extremely complicated, various investigations have been conducted to study certain particular processes mentioned above. Taylor[2] conducted experimental tests to study the convective burning of porous propellants with closed- and open-end boundary conditions. He observed a critical pressure above which the hot gas can penetrate into the porous propellant and significantly increase the regression rate of the charge. He observed the deceleration of the flame front at the closed end of the propellant charge.

Prentice[3] studied the flame-spreading phenomena in transparent solid-propellant cracks using high-speed motion pictures and fine thermocouples. Difficulties were encountered in using fine thermocouples due to the long response time of the thermocouple, uncertainty in the precise locations of the thermocouple, and also due to the gaseous explosion. For closed-end cracks, with small diameters, he observed that the flame cannot propagate into the crack when the bomb pressure is low.

Bobolev et al.[4] studied the mechanism by which combustion products penetrate into the propellant crack. Two mechanisms were proposed: 1) forced penetration of gas due to a higher external pressure, followed by 2) "spontaneous penetration" of product gases from the crack surface into the unburned region of the propellant crack.

Belyaev et al.[5] showed that burning of propellant inside a narrow pore may lead to an excess pressure buildup. Their experimental results have indicated that the erosive burning effect cannot be neglected in the crack combustion study.

In a later study, Belyaev et al.[6] made a series of experimental tests to study the dependence of the flame-spreading rate on crack geometry, propellant properties, boundary conditions, and combustion chamber pressures. They found that both the flame-spreading rate and pressure gradient along a crack are strong functions of crack width. For a closed-end crack, they observed that the flame-spreading rate increases initially until reaching a constant speed and then decelerates near the tip of the crack.

Cherepanov[7] stated that in a sufficiently narrow and long cavity, as a result of the impeded gas flow, the pressure reaches such high values that the system becomes unstable. He further divided the instability mechanism into two different physical forms: 1) local volume burning at the end of the cavity and 2) local destruction of the propellant. In his theoretical analysis, steady-state conditions were assumed, but this is not practical in a real case. The ignition criterion was not established in the analysis, and the continuity equation did not include the mass addition due to burning. Friction loss in the momentum equation was also neglected. Energy release due to combustion and energy loss from the hot gas to the unburned propellant was ignored. Thus, the analysis cannot predict the flame propagation and the actual combustion phenomena inside a propellant crack.

Margolin et al.[8] indicated that the spontaneous penetration of combustion gases into the pores of a gas-permeable explosive charge occurs when the Andreev number (An) is beyond its critical value. The boundary conditions were found to be important in flame propagation. Godai,[9] in his experiment, indicated that a threshold diameter or a critical width of a uniform cavity exists, below which flame will not propagate into the crack.

Krasnov et al.[10] investigated the rate of penetration of combustion into the pores of an explosive charge. The experiment was performed in a constant-pressure bomb. The experimental results showed that the flame-spreading rate is not equal to the rate of penetration of the combustion products into the channel. Their theoretical model was based on the following crude assumptions: 1) constant thermal wave penetration depth in the heated propellant along the flow direction, 2) uniform temperature profile inside the heated propellant layer, and 3) steady-state assumptions for the heat balance equation. Hence, their theoretical approach is inadequate for predicting flame spreading.

Jacobs et al.[11,12] studied the pressure distribution in burning cracks that simulate the separation or debond of solid propellant from the motor casing. Wedge-shaped channels with debond angles of 4.75, 3.17, and 1.90 deg were tested in a combustion chamber at various levels of pre-pressurization. Pressure measurements were obtained at three locations along the debond and at one location in the pressure chamber. The propellant was doped with a highly flammable mixture of titanium and ammonium perchlorate powder so that ignition under increased pressures could be safely assumed to approach that of instantaneous ignition over the entire surface. This ignition procedure was advantageous for them to compare the experimental results with a quasisteady theoretical model. The actual ignition and flame-spreading processes were avoided. Although their analysis may be useful for some cases in the time interval after an extremely rapid ignition process, their model in general cannot be used to predict the overall transient behavior in crack combustion.

Other related studies of combustion inside propellant cracks can be found in the literature.[13,14] Although many interesting experimental results have been obtained, no sound theoretical model was developed. Therefore, the objectives of this work are as follows: 1) to establish a theoretical model for predicting the rate of flame propagation inside a single isolated crack of variable geometry; 2) to predict the pressure distribution and pressurization rate inside a crack, leading to a basis for calculating overall stress loading in the crack; 3) to parametrically investigate the influence of crack geometry, main chamber pressurization rate, and other physicochemical parameters on the gasification rate inside the propellant cavity; and 4) to design and test an experimental combustion chamber for verification of the theoretical model and for establishment of a fundamental data base in crack combustion.

As previously mentioned, the overall problem is extremely complicated. It is not the objective of this paper to model the entire process, but rather to focus only on the combustion aspect, in order to provide a basis for future studies that include crack growth due to stress concentration caused by rapid cavity pressurization.

It is also important to note that although imperfections in solid-propellant grains may be distributed in an irregular intricate network, a rational starting point for understanding the complicated interaction of the above mentioned phenomena is to consider a simple ordered system—a single isolated crack. For such a system, it is desirable to establish a criterion for stable combustion without catastrophic crack propagation; the delineation of a safe domain of governing parameters is the ultimate goal. But before it can be achieved, a realistic theoretical model describing the transient flame-spreading and combustion processes inside a propellant crack has to be established and experimentally verified.

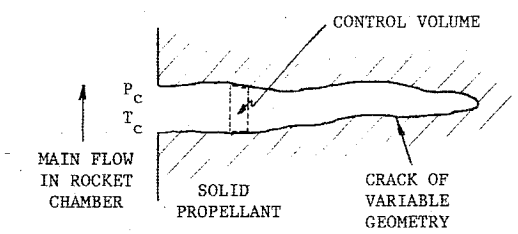

Fig. 1 The physical model of a transverse crack in solid propellant.

II. Analysis

A. Description of the Physical Model

The physical model simulates a transverse propellant crack inside a rocket chamber. It represents a crack located in a transverse direction to the main flow of the rocket chamber and can be of variable geometry to generalize the problem. The physical model is illustrated in Fig. 1.

B. Basic Assumptions

The following basic assumptions are used in the theoretical model:

1) All chemical reactions occur near the propellant crack surface, in a combustion zone that is so thin that it can be considered as a plane. That is, the thickness of the combustion zone above the propellant surface is much smaller than the gap width in the propellant crack.

2) Rate processes at the propellant surface are quasisteady in the sense that the characteristic times associated with the gaseous flame and preheated propellant are short compared to that of the pressure transient variation.

3) The gases flowing in the propellant crack obey the Clausius or Noble-Abel equation of state. This dense gas relation can adequately describe the departure from the ideal gas law at high pressures.

4) The bulk flow in the pore is one-dimensional. Recent experiments conducted by Kuo et al.[15] have revealed that the one-dimensional assumption is appropriate for flow in cracks when the pressure gradient along the crack is greater than a critical value, which normally is extremely small.

5) The compressibility of the solid propellant is neglected. The change of port area in propellant cracks is solely due to the propellant surface regression. The authors recognize that the assumption of negligible propellant deformation may be unrealistic. However, before this effect can be adequately treated, a reliable transient combustion model has to be developed to supply the necessary temporal and spatial pressure distributions required by an appropriate stress-analysis code.

C. Theoretical Modeling

To describe the gas-phase behavior inside a solid-propellant crack, the mass, momentum, and energy equation in unsteady, quasi-one-dimensional forms have been developed based upon the balance of fluxes in a control volume within the propellant crack.

The mass conservation equation is

$$\frac{\partial(\rho A_p)}{\partial t}+\frac{\partial(\rho u A_p)}{\partial x}=r_b\rho_{pr}\mathcal{P}_b \tag{1}$$

The momentum conservation equation is

$$\frac{\partial}{\partial t}(\rho u A_p)+\frac{\partial}{\partial x}(\rho A_p u^2)=-gA_p\frac{\partial P}{\partial x}+g\frac{\partial}{\partial x}(A_p\tau_{xx})$$
$$-\mathcal{P}_w\tau_w g\cos\Theta_w+\rho A_p B_x g-(\rho_{pr}r_b\mathcal{P}_b)V_{gf}\sin\Theta_w \tag{2}$$

The energy conservation equation written in terms of the total stored energy (internal and kinetic) per unit mass, E, is

$$\frac{\partial}{\partial t}(\rho A_p E)+\frac{\partial}{\partial x}(\rho A_p u E)=\frac{\partial}{\partial x}\left(\lambda A_p\frac{\partial T}{\partial x}\right)$$
$$-\frac{1}{J}\frac{\partial}{\partial x}(A_p P u)+\frac{1}{J}\frac{\partial}{\partial x}(\tau_{xx}A_p u)+\rho_{pr}r_b\mathcal{P}_b h_f$$
$$-\bar{h}_{cp}\mathcal{P}_b(T-T_{ps})+\frac{B_x\rho A_p u}{J}-\bar{h}_{cw}(\mathcal{P}_w-\mathcal{P}_b)(T-T_{ws}) \tag{3}$$

The conservation equations are simplified further by an order of magnitude analysis showing that the following terms are negligible: 1) forces between gas molecules due to the viscous normal stress in the axial direction, created by the axial velocity gradient in the momentum equation; 2) viscous dissipation and rate of work done by the force due to viscous normal stresses in the energy equation; and 3) axial heat conduction between gas molecules in the energy equation.

After rearranging the conservation equations, a set of three governing equations is obtained, i.e., velocity-variation, temperature-variation, and pressure-variation equations. These three governing equations are first-order, coupled, inhomogeneous, and nonlinear partial differential equations. The unknowns that vary strongly with respect to the spatial variables are gas temperature, pressure, velocity, and the temperatures at the propellant surface and inert wall. There are other unknown parameters that vary weakly with respect to spatial variables. These parameters include the port area of the crack, the burning rate of the propellant, the convective heat transfer and friction coefficients, the gas flow angle, the local blowing velocity normal to the propellant surface, the wetted perimeter, and the burning perimeter at various locations along the crack.

To solve all the unknowns mentioned above, additional equations and boundary conditions together with some physical input functions must be specified. The propellant surface temperature at a fixed location along the crack before the attainment of ignition is calculated from the solid-phase heat conduction equation which is written in the unsteady one-dimensional form

$$\frac{\partial T_{pr}(t,y)}{\partial t}=\alpha_{pr}\frac{\partial^2 T_{pr}(t,y)}{\partial y^2} \tag{4}$$

where the length variable y is measured perpendicular to the local propellant crack surface. The initial and boundary conditions are

$$T_{pr}(0,y)=T_{pi} \tag{5}$$

$$T_{pr}(t,\infty)=T_{pi} \tag{6}$$

$$\frac{\partial T_{pr}}{\partial y}(t,0)=-\frac{\bar{h}_c(t)}{\lambda_{pr}}[T(t)-T_{ps}(t)] \tag{7}$$

The heat conduction equation is solved either by using an integral method[16] employing a thrid-order polynomial or by direct numerical solution of Eqs. (4-7) with variable mesh size in the subsurface.

For the gas phase, the Noble-Abel equation is used for the equation of state:

$$P(1/\rho-b)=RT \tag{8}$$

For the solid phase, the statement of a constant density for the solid propellant serves as the equation of state.

The expression for the local convective heat-transfer coefficient, $\bar{h}_c$, is deduced from the conventional Dittus-Boelter correlation for turbulent flow in pipes.[17] Variation of the physical properties of the gas across the boundary layer is considered by evaluating the properties at an average film temperature, T_{af}. Before local ignition $\bar{h}_{cp}=\bar{h}_{cw}=\bar{h}_c$, whereas after local ignition $\bar{h}_{cp}=0$ and $\bar{h}_{cw}=\bar{h}_c$. The Prandtl number used in the Dittus-Boelter correlation is calculated from Svehla's equation.[18] The correlation for the friction coefficient used in this study is the modified form of the well-known Colebrook formula,[19] which is discussed in Ref. 17. Zero wall friction is assumed at the burning surface inside the crack due to large friction attenuation caused by the surface blowing.

In the absence of a more adequate erosive burning-rate expression, the Lenoir-Robillard[20] burning-rate formula is used to account for erosive burning effect. After T_{ps} is solved, a simplified ignition temperature criterion is used to determine the burning condition of the solid propellant along the crack. To avoid the step function change in burning rate, a two-temperature criterion is used to achieve full ignition within a finite time interval; when T_{ps} is equal to T_{cri}, the propellant starts to gasify. As soon as T_{ps} reaches T_{ign}, the full ignition condition is reached.

The initial conditions required for the solution of the system of governing equations are

$$u(0,x)=u_i \quad T(0,x)=T_i \quad P(0,x)=P_i \tag{9}$$

where u_i, T_i, and P_i are the initial velocity, temperature, and pressure in the propellant crack.

The number of boundary conditions required depends upon the flow direction and Mach number at the opening of the crack. When the gas in the rocket chamber flows subsonically into the propellant crack, two boundary conditions at the opening of the propellant crack are specified to represent the interface conditions at the crack entrance; and one boundary condition at the closed end of the propellant crack is specified to indicate that the gas velocity is zero. In the mathematical form, they are represented as follows:

$$P(t,0)=P_c(t) \quad T(t,0)=T_c(t) \quad u(t,x_L)=0 \tag{10}$$

When the flow of the gas out of the crack is subsonic, two boundary conditions are specified. They are written as

$$P(t,0)=P_c(t) \quad u(t,x_L)=0 \tag{11}$$

When the outflowing gas is supersonic, only one boundary condition can be specified, that is

$$u(t,x_L)=0 \tag{12}$$

To solve the system of governing equations with a second-order numerical scheme, extraneous boundary conditions are required in addition to the physical ones. The procedure to attain these conditions is discussed in the following section.

D. Numerical Solution Technique

The governing equations, describing the flame-spreading and combustion processes in a propellant crack, were found to be totally hyperbolic.[21] The numerical techniques developed were chosen on the basis of stability, maximum accuracy, and computational efficiency. Recently obtained experience in solving hyperbolic partial differential equations[22] was utilized, and a generalized implicit scheme[23] based on central differences in spacewise derivatives was chosen to solve the governing equations. A quasilinearization method, used to linearize the inhomogeneous terms in the governing equation, was combined with a stable predictor-corrector procedure.[17] Finally, the governing equations, in their finite-difference form, are arranged in a block-tridiagonal matrix form,[17] which allows an efficient computation.

The use of central difference formulation for all spacewise derivatives in the governing equations require six boundary conditions for the solution. This implies that, when the gas flows into the crack, three extraneous boundary conditions are required in addition to the three physical ones described by Eq. (10). The three extraneous boundary conditions are used to determine the flow velocity at the opening of the crack, and the pressure and temperature at the closed end of the crack.

When the gas flows out of the crack subsonically, in addition to the two physical boundary conditions described in Eq. (11), two extraneous boundary conditions are required at the opening of the crack for the determination of the pressure and temperature. Also, two extraneous boundary conditions are required at the closed end of the crack.

When the outflowing gas is supersonic, in addition to the physical boundary condition given by Eq. (12), three extraneous boundary conditions are needed at the opening of the crack and two other extraneous boundary conditions are needed at the tip of the crack.

These extraneous boundary conditions for the hyperbolic system of governing equations are derived from the compatibility relations at the boundaries. The relations are obtained by transforming the governing equations using the method of characteristics.[17] The compatibility relations together with the physical boundary condition form a closed system to determine the velocity, temperature, and pressure at both ends of the crack.

III. Experimental Apparatus and Procedure

A. Test Rig Design

The design of this test rig was guided by the following primary considerations: 1) The experimental set-up should be as close as possible to the physical conditions considered in the analytical model so that the experimental results can be used directly for the verification of the theoretical solutions. 2) The test rig should have sufficient flexibility to permit a wide range of variation in propellant crack geometry, properties, chamber pressure, pressurization rate, igniter gas temperature, and the main-chamber mass flow rate in the transverse direction to the crack. This flexibility in testing is essential for the establishment of a fundamental data base in propellant crack combustion.

A schematic diagram of the test rig is shown in Fig. 2, and an assembly view of the propellant crack combustion chamber is shown in Fig. 3. The propellant containing a simulated crack is cast into a brass mold. A special mandrel is used during the propellant molding process to produce a 2.54-cm-deep channel-shaped crack of length L and gap width δ. In this paper, two different crack geometries have been used. For the large crack, $L=20$ cm and the average $\delta=0.52$ cm. For the small crack, $L=15$ cm and the average $\delta=0.08$ cm. The main block of the combustion chamber has five parts machined into its backside along the longitudinal axis of the crack to accept four piezoelectric pressure transducers and a safety burst diaphragm. The pressure transducers are located at distances of 0.0, 4.8, 13.8, and 18.8 cm from the initial crack opening. The window assembly consist of a ¼-in. sacrificial

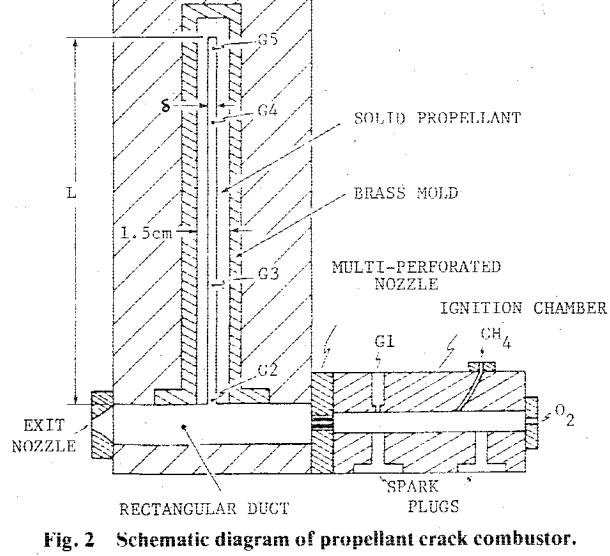

Fig. 2 Schematic diagram of propellant crack combustor.

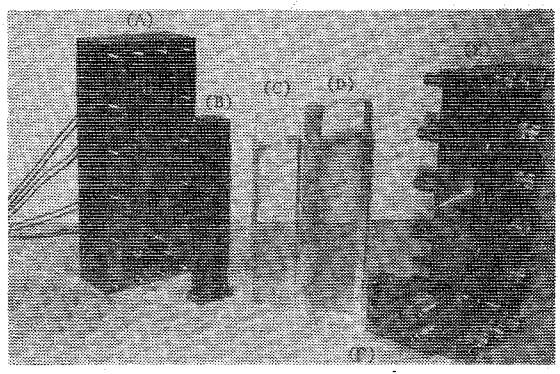

Fig. 3 Assembly view of the combustion chamber: (A) main chamber block, (B) brass mold containing propellant-crack specimen, (C) sacrificial window, (D) main window, (E) window retainer, (F) interchangeable exit nozzle.

Plexiglas plate and a main Plexiglas window. This window assembly, along with a stainless-steel retainer, is used to close the combustion chamber and permit visual recording of the luminous flame front inside the propellant crack. An interchangeable exit nozzle is connected to the combustion chamber for control of the rate of chamber pressurization. The combustion chamber was designed for a maximum static pressure of 800 atm.

An ignition system has been developed using spark plugs to ignite a gaseous mixture of oxygen and methane. Both fuel and oxidizer feed-lines contain a pressure regulator and critical flow orifice that permit exact control of the fuel-oxidizer flow rates. The gaseous reactants are first mixed in the igniter chamber by tangentially injecting methane into the oxygen flowstream. The mixed reactants then enter the test section through a multiperforated convergent nozzle. This versatile igniter design provides the necessary variability to produce a wide range of igniter strength.

B. Test Procedure

A typical test firing is conducted in the following manner. To prevent unburned igniter gases from entering the crack, a strip of tape is used to cover the entrance of the crack. The fuel and oxidizer flow rates are set to predetermined values. As the cold igniter gases pass over the sealed crack entrance, a high-speed camera is turned on. A timing signal is then activated which places light pulses on the film and simultaneously sends a pulse to the tape recorder to synchronize the film with the pressure data on the tape. Ignition is then achieved with two conventional autombile spark plugs. Hot igniter gases pass from the ignition chamber through a multiperforated nozzle to the combustion chamber; the tape covering the crack entrance burns away immediately and the hot gases enter the crack. After an induction interval, the propellant at the crack entrance reaches ignition condition. The flame spreading process is then observed by the 16-mm high-speed camera. The pressurization process in the propellant crack is simultaneously recorded on the magnetic tape.

IV. Discussion of Results

A. Comparison of Theoretical Results with Experimental Data

A number of test firings with a smokeless propellant have been conducted in the crack combustion facility. The larger crack ($\delta \equiv 0.5$ cm) was used during the phase of initial system checkout. The experimental results of a smaller crack, having a length of 15 cm and a gap width of 0.051 cm at the entrance with a gradual increase to 0.107 cm at the tip, are discussed herein. (Although we call the above configuration a "small" crack, the gap width may be an order of magnitude larger than that of the actual cracks found in rocket grains.)

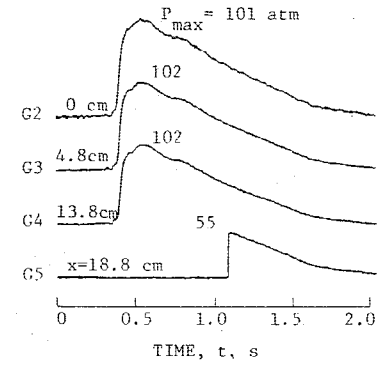

Fig. 4 Experimental pressure-time traces from DNC test no. 11.

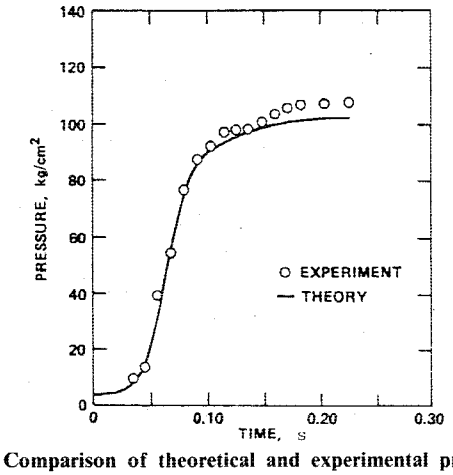

Fig. 5 Comparison of theoretical and experimental pressure-time profiles at $x = 4.8$ cm.

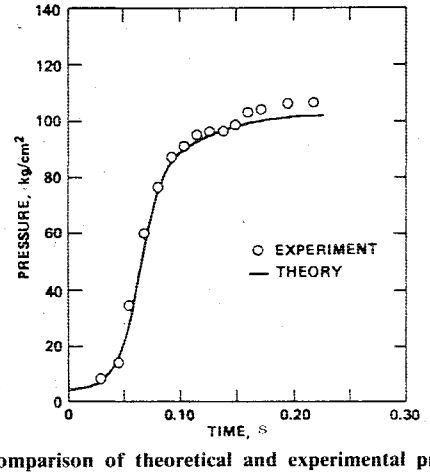

Fig. 6 Comparison of theoretical and experimental pressure-time profiles at $x = 13.8$ cm.

Typical pressure-time traces recorded from a test firing of a "small" crack configuration are shown in Fig. 4. G2 represents the pressure history at the entrance of the crack. G5 was initially covered by the propellant specimen and therefore senses pressure at a later time. In this test, a large exhaust nozzle was used to produce a relatively low pressurization rate at the crack entrance. This resultant pressurization rate is close to the typical value obtained during the starting transient of many rocket motors. An examination of the G2–G4 pressure-time traces reveals that the spatial pressure gradient inside the crack is very low. This nearly uniform spatial pressure history is due to the relatively low value of dPc/dt and to a significantly large gap width; these conditions are favorable for the reduction of pressure wave phenomena. As

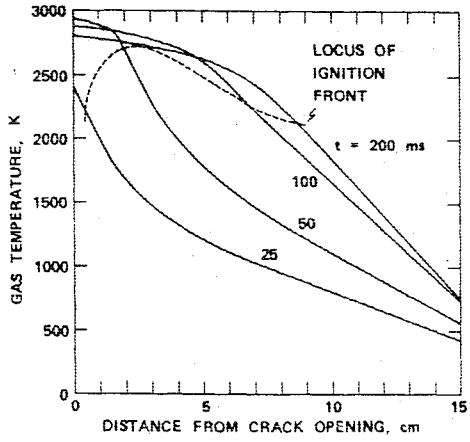

Fig. 7 Calculated gas temperature distribution for various times.

shown in Figs. 5 and 6, the predicted pressure-time profiles at two stations inside the crack are in close agreement with the experimental data. In this test an exceedingly long induction period was required for the igniter gases to burn away the protective tape and establish ignition at the crack entrance. Consequently, no useful flame-spreading data were obtained. However, in another firing with nearly identical test conditions, the luminous flame front was found to propagate slowly near the crack entrance and then suddenly accelerate to a nearly uniform velocity. A similar behavior in the flame-spreading rate was also observed experimentally by Belyaev et al.[6]

Figure 7 describes the calculated gas temperature distribution along the crack at various times. Because of the high flame temperature and short transient times, no attempt was made to measure the gas temperature inside the crack. The input data used to make these predictions are listed in Table 1. The locus of the calculated ignition front is superimposed on this figure. The gradient in the temperature distribution is very pronounced, indicating the penetration of hot gases into the propellant crack. For times greater than 50 ms, the gas temperature at the opening portion of the crack decreases slightly; this is mainly due to outflow of product gases.

Figure 8 shows the calculated gas velocity profiles that exist in the small crack at various times. At a time of 1 ms, the hot gases are flowing into the crack at a high velocity because of a large initial pressure gradient. At 25 ms the velocity of the inflowing gases decreases as the pressure distribution along

Table 1 Computer program input variables

x_p	$=0.0$ cm
x_L	$=15.05$ cm
B_x	$=0.0\,g_f/g$
b	$=1.0\,cm^3/g$
M_w	$=23.97\,g_f$/g-mole
γ	$=1.233$
ρ_{pr}	$=1.741\,g/cm^3$
λ_{pr}	$=0.44\times10^{-3}$ cal/s-cm-K
α_{pr}	$=0.0011\,cm^2/s$
ϵ_s/d_h	$=0.001$
T_f	$=3000$ K
T_{cri}	$=780$ K
T_{ign}	$=1000$ K
T_i	$=298$ K
a	$=2.752\times10^{-4}$ (cm/s)/(g_f/cm^2)^n
n	$=0.683$
K_e	$=15.9\,cm^3$-K/cal
β	$=125$
T_c	$=2800$ K

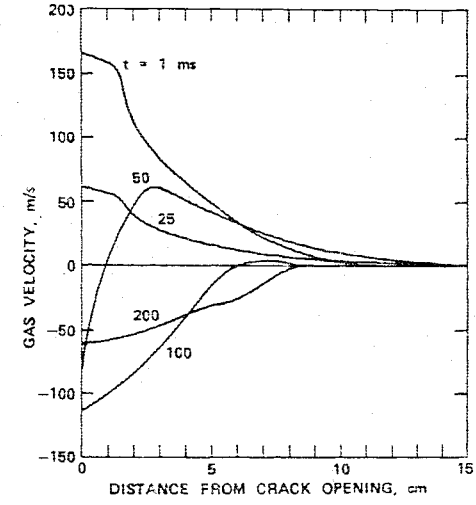

Fig. 8 Calculated velocity distribution at various times.

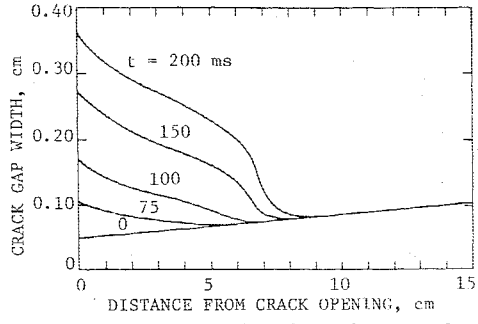

Fig. 9 Calculated growth of crack gap due to combustion.

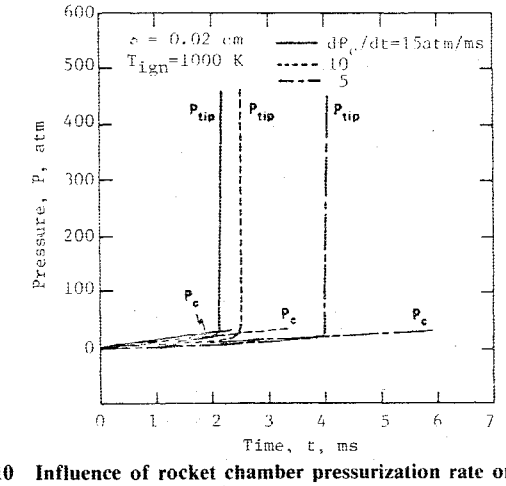

Fig. 10 Influence of rocket chamber pressurization rate on the internal pressurization process inside a narrow crack ($\delta = 0.02$ cm).

the crack becomes more uniform. A negative velocity is obtained at 50 ms in a region near the crack opening, which indicates an outflow of product gases. As the flame front progresses along the crack, the resultant gasification processes cause an increase in velocity of the gases flowing out of the crack. Due to the large increase in port area at the opening of the crack (see Fig. 9), the velocity of the outflowing gases decrease between 100 and 200 ms. During the entire pressurization process, the gas velocity near the closed end of the crack is very low; this is due to the lack of a favorable pressure gradient. This very low flow velocity causes a significant reduction in the convective heating of the propellant surface. Hence, a much longer time is required for the propellant surface near the crack tip to achieve a state of ignition.

B. Parametric Study

A parametric study was conducted with the theoretical model to determine the influence of variations in chamber pressurization rate, crack gap width, and ignition parameters on the flame spreading and resultant pressurization inside propellant cracks. Unless otherwise described, the input constants used in this theoretical study are given in Table 1.

Figure 10 describes the pressure history at the tip of a small constant-area crack ($\delta = 0.02$ cm) for various chamber pressurization rates. Three sets of curves are shown in this plot for dPc/dt varying from 0.5×10^4 to 1.5×10^4 atm/s. Each set of curves compares the calculated pressurization history at the tip of the crack with the assumed chamber pressure variation. As shown in this plot, the pressurization rate at the tip of the crack changes abruptly due to the gasification of propellant surface inside the crack. The time required to attain this "rapid pressurization" is aptly designated as t_{RP}.

This time can either be defined as the time when the pressure at the crack tip exceeds the chamber pressure, or when the two tangent lines, drawn on each side of the curve describing the rapid pressure transition, intersect. For small cracks and large dPc/dt, both methods for obtaining t_{RP} are nearly equivalent. As shown in Fig. 10, t_{RP} decreases for increasing chamber pressurization rates. This trend is mainly due to the increase of forced convection driven by a large streamwise pressure gradient. This augmentation in the rate of convective heat transfer significantly enhances the rate of flame spreading and surface gasification.

A similar study is shown in Fig. 11 for a larger crack ($\delta = 0.05$ cm). Because of the large gap width, a very-low-pressure gradient prevails along the crack. This causes the crack tip pressure to closely track the chamber pressure before appreciable surface gasification. For this particular case, t_{RP} is more adequately defined by the tangent-intersection method. Similar to the small-crack results, the theoretical predictions for this large crack reveal that a larger delay in t_{RP} is experienced when dPc/dt is reduced.

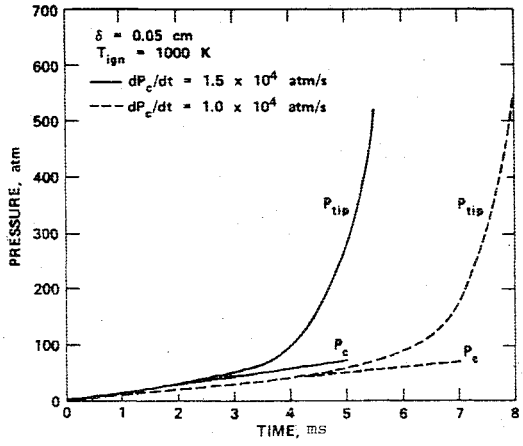

Fig. 11 Influence of rocket chamber pressurization rate on the internal pressurization process inside a wide crack ($\delta = 0.05$ cm).

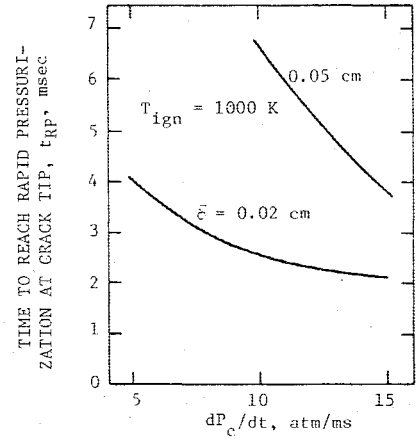

Fig. 12 Influence of gap width and rocket chamber pressurization rate on the time to reach rapid pressurization at crack tip.

The combined effects of gap width and chamber pressurization rate are shown in Fig. 12. This cross-plot indicates that the time required to reach rapid pressurization at the crack tip becomes shorter with a decrease in the gap width and with an increase in the rocket chamber pressurization rate. For very large cracks, the definition of t_{RP} become less clear and difficult to interpret. For extremely small cracks, there is a critical gap width below which a flame cannot easily propagate; therefore, t_{RP} will increase significantly with further reduction in gap width.

The influence of propellant ignition temperature on the time to reach rapid pressurization at the crack tip, t_{RP}, is also studied for various rates of chamber pressurization. It is found that t_{RP} for this small crack ($\delta = 0.02$ cm) diminishes with a reduction in the ignition temperature. In addition, the flame-spreading and pressurization processes inside a crack of a given initial geometry become less sensitive to the propellant ignition temperature as the forced convection becomes stronger.

V. Conclusions

1) A one-dimensional theoretical model has been developed to describe the transient combustion phenomena in a propellant crack. The theoretical model can be used to predict wave phenomena, heat transfer from the gas to the propellant surface and associated thermal penetration, and flame propagation and resultant pressurization at various locations along the propellant cavity.

2) For cracks with a gap width above the critical value required for gas penetration, the internal pressurization rate, pressure gradient, and flame velocity in the crack increase as the gap width decreases, the rocket chamber pressurization rate increases, and the propellant ignition temperature decreases.

3) During the early phase of flame spreading, pressure wave phenomena exist and the crack pressurization rate is controlled by the rocket chamber conditions. At a later time, the cavity pressurization is dominated by propellant combustion.

4) The calculated flame front deceleration near the crack tip agrees with experimental observations made separately by Taylor[2] and Belyeav et al.[6]

Acknowledgment

This paper represents the results of research begun under Hercules Contract No. 0270-05122 and continued under U.S. Navy contract at Department of Mechanical Engineering, The Pennsylvania State University. The advice of M. W. Beckstead of Hercules Inc., Magna, Utah, and R. L. Derr and C. F. Price of the Aerothermochemistry Division of N.W.C., China Lake, California, are greatly appreciated. The authors would also like to acknowledge D. R. McClure of Dahlgren Lab of N.S.W.C for his help in experimental test firings and numerical computations.

References

[1] Malik, D. F., "Storage Reliability of Missile Material Program, Solid Propellant Rocket Motor Analysis," Raytheon Company, Huntsville, Ala., Report LC-76-0R1 (also DDC Report AD-A026105), May 1976.

[2] Taylor, J. W., "The Burning of Secondary Explosive Powders by a Convective Mechanism," *Transactions of the Faraday Society*, Vol. 58, 1962, p. 561.

[3] Prentice, J. L., "Flashdown in Solid Propellants," U.S. Naval Ordinance Test Station, China Lake, Calif., NAVWEPS Rept. 7964, NOTS TP 3009, Dec. 1962.

[4] Bobolev, V. K., Margolin, A. D., and Chuiko, S. V., "The Mechanism by Which Combustion Products Penetrate into the Pores of a Charge of Explosive Material," *DokLady Akademii Nauk USSR*, Vol. 162, May 1965, pp. 388-391.

[5] Belyaev, A. F., Korotkov, A. I., Sulimov, A. A., Sukoyan, M. K., and Obmenin, A. V., "Development of Combustion in an Isolated Pore," *Combustion, Expolsion and Shock Waves*, Vol. 5, Jan.-March 1969, pp. 4-9.

[6] Belyaev, A. F., Bobolev, V. K., Korotkov, A. I., Sulimov, A. A., and Chuiko, S. V., "Development of Burning in a Single Pore," *Transition of Combustion of Condensed Systems to Detonation*, Chap. 5, Pt. A, Sec. 22, Science Publisher, 1973, pp. 115-134.

[7] Cherepanov, G. P., "Combustion in Narrow Cavities," *Journal of Applied Mechanics and Technical Physics*, Vol. 11, 1970, pp. 276-281.

[8] Margolin, A. D. and Margulis, V. M., "Penetration of Combustion into an Isolated Pore in an Explosive," *Combustion, Explosion and Shock Waves*, Vol. 5, Jan.-March 1969, pp. 15-16.

[9] Godai, T., "Flame Propagation into the Crack of a Solid-Propellant Grain," *AIAA Journal*, Vol. 8, July 1970, pp. 1322-1327.

[10] Krasnov, Yu. K., Margulis, V. M., Margolin, A. D., and Pokhil, P. F., "Rate of Penetration of Combustion into the Pores of an Explosive Charge," *Combustion, Explosion, and Shock Waves*, Vol. 6, July-Sept. 1970, pp. 262-265.

[11] Jacobs, H. R., Williams, M. L., and Tuft, D. B., "An Experimental Study of the Pressure Distribution in Burning Flaws in Solid Propellant Grains," University of Utah, Salt Lake City, Utah, Final Report to Air Force Rocket Propulsion Laboratory, AFRPL-TR-72-108, UTEC DO 72-130, Oct. 1972.

[12] Jacobs, H. R., Hufferd, W. L., and Williams, M. L., "Further Studies of the Critical Nature of Cracks in Solid Propellant Grains," AFRPL-TR-75-14, March 1975.

[13] Belyaev, A. F., Sukoyan, M. K., Korotkov, A. I., and Sulimov, A. A., "Consequences of the Penetration of Combustion into an Individual Pore," *Combustion, Explosion and Shock Waves*, Vol. 6, April-June 1970, pp. 149-153.

[14] Franics, E. C., Lindsey, G. H., and Parmerter, R. R., "Pressurized Crack Behavior in Two-Dimensional Rocket Motor Geometries," *AIAA Journal*, Vol. 9, June 1972, pp. 415-419.

[15] Kuo, K. K., Chen, A. T., and Davis, T. R., "Transient Flame Spreading and Combustion Processes inside a Solid Propellant Crack," AIAA Paper 77-14, AIAA 15th Aerospace Sciences Meeting, Jan. 1977.

[16] Goodman, T. R., "Application of Integral Methods to Transient Nonlinear Heat Transfer," *Advances in Heat Transfer*, Vol. 1, Academic Press, New York, 1964, pp. 51-122.

[17] Peretz, A., Kuo, K. K., Caveny, L. H., and Summerfield, M., "Starting Transient of Solid-Propellant Rocket Motors with High Internal Gas Velocities," *AIAA Journal*, Vol. 11, Dec. 1973, pp. 1719-1727.

[18] Svehla, R. A., "Estimated Viscosities and Thermal Conductivities of Gases at High Temperatures," NASA TR R-132, 1962.

[19] Colebrook, C. F., "Turbulent Flow in Pipes with Particular Reference to the Transition Region Between the Smooth and Rough Pipe Laws," *Journal of the Institute of Civil Engineers*, Vol. 11, 1938-39, pp. 133-156.

[20] Lenoir, J. M. and Robillard, G., "A Mathematical Method to Predict the Effects of Erosive Burning in Solid Propellant Rockets," *6th Symposium (Int.) on Combustion*, 1956, pp. 663-667.

[21] Courant, R. and Hilbert, D., *Methods of Mathematical Physics*, Vol. 2, Interscience Publishers, New York, July 1966, pp. 407-550.

[22] Kuo, K. K., "Theory of Flame Front Propagation in Porous Propellant Charges under Confinement," Ph.D. Thesis, AMS Report T-1000, Princeton University, Princeton, N.J., Aug. 1971.

[23] Richtmyer, R. D. and Morton, D. W., *Difference Methods for Initial-Value Problems*, Interscience Publishers, New York, 1967.

From the AIAA Progress in Astronautics and Aeronautics Series . . .

RADIATION ENERGY CONVERSION IN SPACE—v. 61

Edited by Kenneth W. Billman, NASA Ames Research Center, Moffett Field, California

The principal theme of this volume is the analysis of potential methods for the effective utilization of solar energy for the generation and transmission of large amounts of power from satellite power stations down to Earth for terrestrial purposes. During the past decade, NASA has been sponsoring a wide variety of studies aimed at this goal, some directed at the physics of solar energy conversion, some directed at the engineering problems involved, and some directed at the economic values and side effects relative to other possible solutions to the much-discussed problems of energy supply on Earth. This volume constitutes a progress report on these and other studies of SPS (space power satellite systems), but more than that the volume contains a number of important papers that go beyond the concept of using the obvious stream of visible solar energy available in space. There are other radiations, particle streams, for example, whose energies can be trapped and converted by special laser systems. The book contains scientific analyses of the feasibility of using such energy sources for useful power generation. In addition, there are papers addressed to the problems of developing smaller amounts of power from such radiation sources, by novel means, for use on spacecraft themselves.

Physicists interested in the basic processes of the interaction of space radiations and matter in various forms, engineers concerned with solutions to the terrestrial energy supply dilemma, spacecraft specialists involved in satellite power systems, and economists and environmentalists concerned with energy will find in this volume many stimulating concepts deserving of careful study.

690 pp., 6×9, illus., $24.00 Mem. $45.00 List

TO ORDER WRITE: Publications Dept., AIAA, 1290 Avenue of the Americas, New York, N. Y. 10019